CONFRONTING THE DAMPING OF THE BARYON ACOUSTIC OSCILLATIONS WITH OBSERVATIONS

Hidenori Nomura, Kazuhiro Yamamoto

Graduate School of Science, Hiroshima University, Higashi-Hiroshima, 739-8526 Japan

Gert Hütsi

Department of Physics and Astronomy, University College London, London, WC1E 6BT, UK
Tartu Observatory, EE-61602 Tõravere, Estonia

Takahiro Nishimichi

Department of Physics, School of Science, The University of Tokyo, Tokyo 113-0033, Japan

Abstract

We investigate the damping of the baryon acoustic oscillations in the matter power spectrum due to the quasinonlinear clustering and redshift-space distortions in a semi-analytic way. This demonstrates that the damping is closely related to the growth factor and the amplitude of the matter power spectrum. Thus, the precise measurement of the damping might be useful in determining the the growth factor and the amplitude of the matter power spectrum in future. We also investigate the damping by confronting the models with the observations of the Sloan Digital Sky Survey luminous red galaxy sample. The chi-squared test suggests that the observed power spectrum is better matched by models with the damping of the baryon acoustic oscillations rather than the ones without the damping.

Joint Subaru/Gemini Science Conference, Kyoto 2009

§1. INTRODUCTION

The baryon acoustic oscillations (BAO), the sound oscillations of the primeval baryon-photon fluid prior to the recombination epoch, left its signature in the matter power spectrum [1,2]. The BAO signature in the galaxy clustering has recently attracted remarkable attention as a powerful probe for exploring the nature of the dark energy component commonly believed to be responsible for the accelerated expansion of the universe [3–6]. The usefulness of the BAO to constrain the dark energy has been demonstrated, and a lot of the BAO survey projects are in progress, or planned [7–9].The BAO signature in the matter clustering plays a role of the standard ruler, because the characteristic scale of the BAO is well understood within the cosmological linear perturbation theory as long as the adiabatic initial density perturbation is assumed.

However, the comparison of the BAO signature with observation is rather complicated. The observed galaxy power spectrum is contaminated by the nonlinear evolution of the density perturbations, the redshift-space distortions and the clustering bias. This enables us to use the galaxy power spectrum for other supplementary tests, in addition to the test of the expansion history of the universe for the equation of state of the dark energy. For example, the redshift-space distortions probe the linear growth rate of the density fluctuations [10,11]. The growth rate is now recognised to be very important as the test of gravity on the cosmological scales.

In this work, we investigate how the quasi-nonlinear density perturbations and redshift-space distortions affect the BAO signature. Especially, we focus on the damping of the BAO signature. The semi-analytic investigation on the basis of the third-order perturbation theory demonstrated that the BAO damping is sensitive to the growth factor $D_1(z)$ and the amplitude of the matter power spectrum σ_8. Here z is the redshift and the growth factor is normalised as $D_1(z) = a$ at $a \ll 1$, where a is the scale factor normalised as $a = 1$ at the present epoch. As a result, a measurement of the BAO damping might be useful as an additional consistency test by enabling one to probe the growth factor multiplied by the amplitude of the matter perturbation $D_1(z)\sigma_8$. We also investigate the damping by confronting the theoretical model with the observation of the Sloan Digital Sky Survey (SDSS) luminous red galaxy (LRG) sample.

§2. DAMPING OF THE BAO - STANDARD PERTURBATION APPROACH

We consider the matter fluctuations after the recombination whose wavelength of interest is smaller than the horizon size, then the evolution of the matter fluctuations can be analyzed by the pressure-less nonrelativistic fluid. Employing the standard perturbation theory (SPT) of the density fluctuations, the second-order matter power spectrum at the redshift z is given,

$$P_{\rm SPT}(k,z) = D_1^2(z)P_{\rm lin}(k) + D_1^4(z)P_2(k), \tag{1}$$

where $D_1(z)$ is the growth factor, $P_{\rm lin}(k)$ is the linear matter power spectrum at the present epoch, and $P_2(k)$ is the second-order contribution to the power spectrum, whose expression is given

$$P_2(k) = P_{22}(k) + 2P_{13}(k). \tag{2}$$

with

$$P_{22}(k) = \frac{k^3}{392\pi^2}\int_0^\infty dr P_{\rm lin}(k)\int_{-1}^{+1} dx P_{\rm lin}(k\sqrt{1+r^2-2rx})\frac{(3r+7x-10rx^2)^2}{(1+r^2-2rx)^2} \tag{3}$$

$$2P_{13}(k) = \frac{k^3}{504\pi^2}P_{\rm lin}(k)\int_0^\infty dr P_{\rm lin}(kr)\left[\frac{12}{r^2} - 158 + 100r^2 - 42r^4\right. \tag{4}$$

$$\left. + \frac{3}{r^3}(r^2-1)^3(7r^2+2)\ln\left|\frac{1+r}{1-r}\right|\right]. \tag{5}$$

The BAO signature in the matter power spectrum can be extracted as follows:

$$B(k,z) \equiv \frac{P(k,z)}{\tilde{P}(k,z)} - 1, \tag{6}$$

where $P(k,z)$ is the matter power spectrum including the BAO signature, but $\tilde{P}(k,z)$ is the matter power spectrum without the BAO. Figure 1 shows $B_{\rm SPT}(k,z)$ as a function of the wavenumber k for several redshifts, which is obtained using the second-order power spectrum $P_{\rm SPT}(k,z)$. One can see the damping of the amplitude of the BAO as the redshift becomes small. In addition, this damping is more significant as the wavenumber k is larger.

The damping of the BAO signature is expressed in terms of the function $W(k,z)$, defined by

$$B(k,z) = [1 - W(k,z)]B_{\rm lin}(k), \tag{7}$$

where $B_{\rm lin}(k)$ is the BAO signature within the linear theory of density fluctuations. With the use of the second-order power spectrum $P_{\rm SPT}(k,z)$, we find the approximate formula for the damping function

$$W(k,z) \simeq D_1(z)^2 \frac{\widetilde{P}_{22}(k)}{\widetilde{P}_{\rm lin}(k)} \simeq D_1(z)^2 \sigma_8^2 \left(\frac{k}{k_n}\right)^2 \left(1 - \frac{\gamma}{k}\right) \tag{8}$$

where

$$k_n = -1.03(\Omega_m h^2 + 0.077)(\Omega_b h^2 - 0.24)(n_s + 0.92) \;\; h{\rm Mpc}^{-1}, \tag{9}$$

$$\gamma = -11.4(\Omega_m h^2 - 0.050)(\Omega_b h^2 - 0.076)(n_s - 0.34) \;\; h{\rm Mpc}^{-1}. \tag{10}$$

Figure 2 compares the theoretical prediction of $B(k,z)$ with the results from the N-body simulations [15]. In the N-body simulation, we adopt a ΛCDM model with the WMAP5 best fit value parameters, 512^3 particles in periodic cubes with each side $1000h^{-1}$Mpc. We apply a method to correct the deviation from the ideal case of infinite volume (see [15] for details). This demonstrates that the approximate formula reproduces the result of N-body simulation for $k \lesssim 0.2$ hMpc^{-1} until $z \sim 1$ within error bars, roughly.

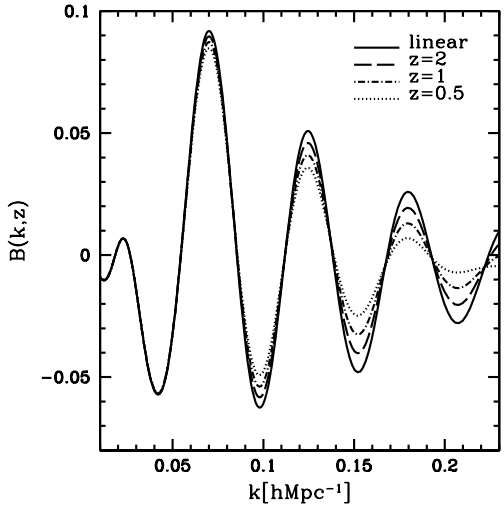

FIG. 1. The BAO signature, $B(k,z)$, as a function of k for several redshifts, $z = 2,\ 1,\ 0.5$, which are derived from the matter power spectrum including the second order contributions. The solid curve is the linear theory. Here the cosmological parameters are $h = 0.7$, $\Omega_m = 0.28$, $\Omega_b = 0.046$, $n_s = 0.96$ and $\sigma_8 = 0.82$.

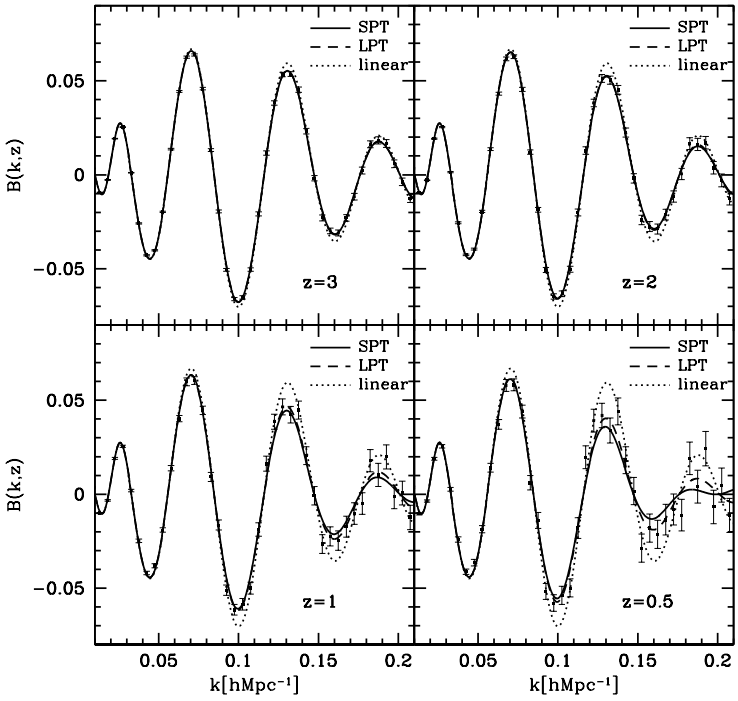

FIG. 2. The square with the error bar is the result of N-body simulation. The solid curve is the fitting formula based on the SPT, while the dotted curve is the linear theory. The dashed curve is the result of an extended fitting formula with the LPT with fixed $\mu = 0$ (see also §3).

§3. DAMPING OF THE BAO - REDSHIFT SPACE

The higher-order nonlinear effect and the redshift-space distortion may affect the damping of the BAO signature. As an alternative to the SPT, we next adopt the framework proposed by Matsubara [14], which uses the technique of resumming infinite series of higher order perturbations on the basis of the Lagrangian perturbation theory (LPT). One of the advantages of using the LPT framework is the ability to calculate the quasi-nonlinear matter power spectrum in redshift-space. In the framework of the LPT [14], the matter power spectrum is rather complicated (see Appendix), but we have the approximate formula for the damping

$$W(k,\mu,z) \simeq \frac{D_1(z)^2}{1+\alpha(\mu,z)D_1^2(z)\tilde{g}(k)} \frac{\widetilde{P}_{22}^{(\mathrm{s})}(k,\mu,z)}{\widetilde{P}_{\mathrm{lin}}^{(\mathrm{s})}(k,\mu,z)} \tag{11}$$

where the tilde means without the BAO, and

$$\alpha(\mu,z) = 1 + f(f+2)\mu^2, \qquad \text{and} \qquad f = \frac{d\ln D_1}{d\ln a}.$$

We consider the angular averaged power spectrum, which is used in measuring the BAO signature in practice. Figure 3 shows a comparison of the theoretical prediction of the LPT formula with the results from the N-body simulations. One can see the agreement between the N-body result and the theoretical prediction.

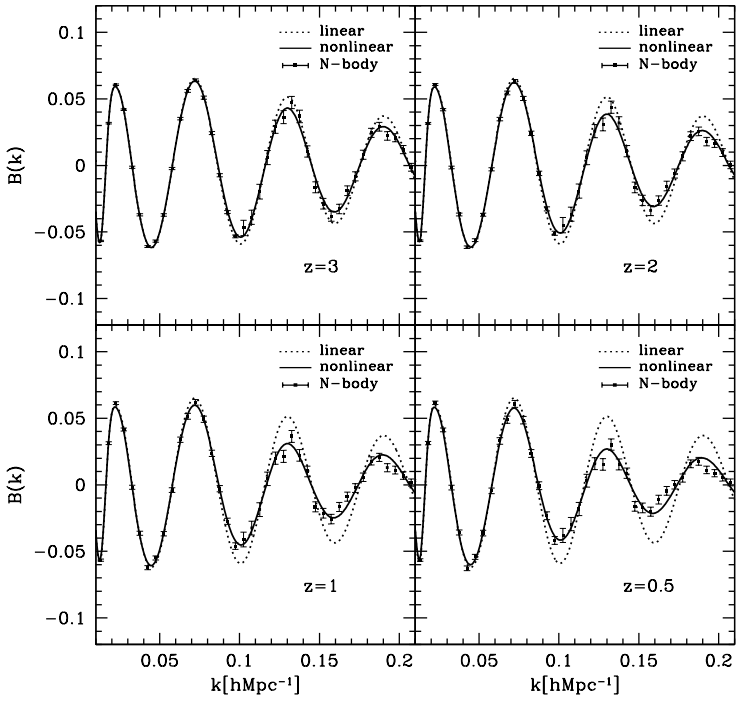

FIG. 3. Comparisons between the theoretical BAO signature and the results from the N-body simulation (squares with error bars) at $z = 3,\ 2,\ 1,\ 0.5$, respectively. The solid curve is the LPT formula and the dotted curve is the linear theory. The solid line is the BAO distorted by the nonlinear redshift-space distortions. The cosmological parameters adopted in this comparison are $h = 0.7$, $\Omega_m = 0.28$, $\Omega_b = 0.046$, $n_s = 0.96$ and $\sigma_8 = 0.82$

§5. COMPARISON WITH THE SDSS LRG POWER SPECTRUM

Now we confront the theoretical predictions with observations. In particular, we use the SDSS LRG sample from Data Release 6. The overall shape of the power spectrum from the LPT formula doesn't match the observational power spectrum. The power spectrum of the LPT formula shows the exponential suppression at large wavenumbers, This feature can be understood as the nonlinear redshift-space distortion [14], the so-called Finger-of-God effect

Then, we first construct the theoretical power spectrum by multiplying the LPT power spectrum by the function $b_0^2 e^{\alpha k^2}$ so as to match the SDSS LRG power spectrum,

$$P_{\rm fit}(k) = b_0^2 e^{\alpha k^2} P^{\rm (s)}_{\rm LPT}(k), \tag{12}$$

where b_0 and α are the fitting parameters. Figure 4 demonstrates example $P_{\rm fit}(k)$, whose parameters are described in the Table I, labelled as the model No.1. One can see that this fitting function matches the observed power spectrum well. We also note that the BAO signature extracted using $P_{\rm fit}(k)$ is not sensitive to the choice of b_0 and α.

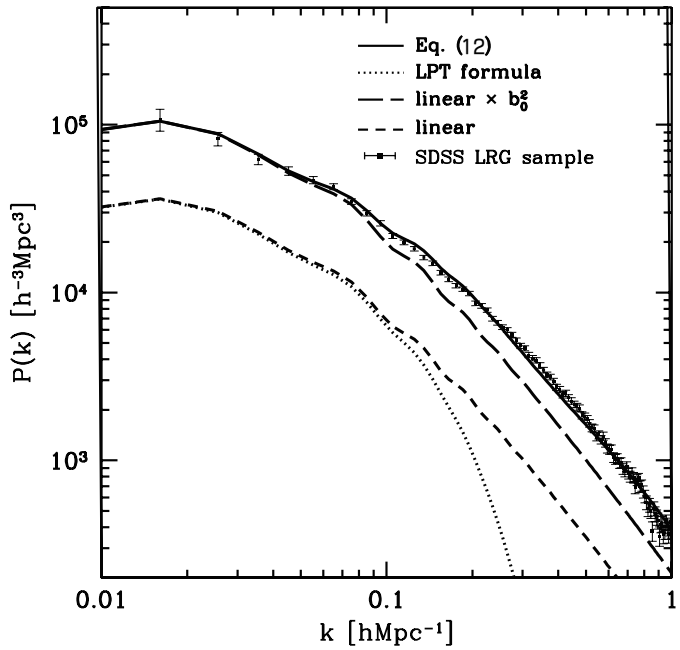

FIG. 4. Comparison of the theoretical power spectra and the SDSS LRG power spectrum.The dotted curve is the LPT formula and the short-dashed curve is the linear theory. The solid curve is the power spectrum multiplied by the correction factor, (12). The long-dashed curve is the linear theory multiplied by the constant b_0^2. The cosmological and fitting parameters are described in Table I labelled as the model No.1.

Figure 5 compares the BAO signatures extracted from the theoretical models and the SDSS LRG power spectrum of Fig. 4. Here we utilise the cubic spline fit to *consistently* construct the smooth component for both the theoretical and the observational power spectra.

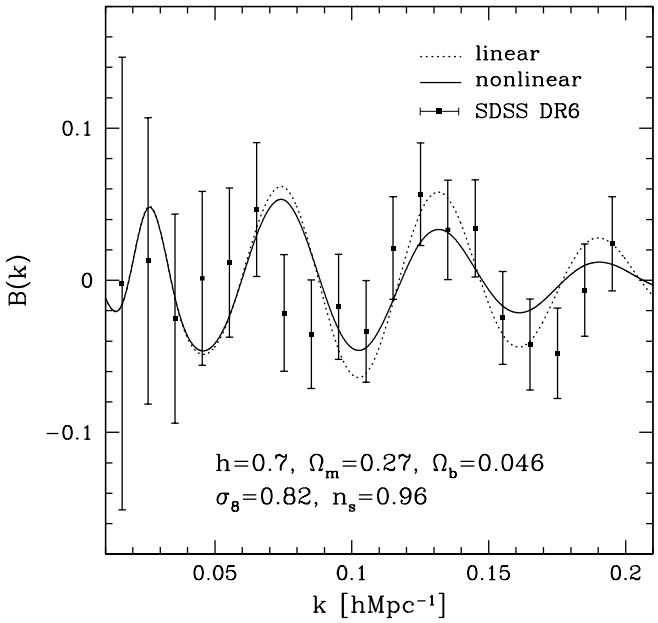

FIG. 5. Comparison of the BAO features extracted from theoretical models and from the observational data. The dotted curve is the linear theory and the solid curve is the LPT result. The squares with the error bars are the results from the SDSS LRG sample. The chi-squared score for this example is listed in the Table I, labelled as the model No.1.

We computed the chi-square as

$$\chi^2 = \sum_i \frac{[B^{\rm th}(k_i) - B^{\rm ob}(k_i)]^2}{\Delta B(k_i)^2}, \tag{13}$$

where $B^{\rm th}(k_i)$ and $B^{\rm ob}(k_i)$ are the theoretical and observational BAO signatures at wavenumber k_i, respectively, and $\Delta B(k_i)$ is the error. In the computation, we used the data in the wavenumber range of $0.015 \leq k \leq 0.195$. The values of the chi-squared test for various cosmological models are listed in Table I.

Here $\chi^2_{\rm LPT}$ is the result for the theoretical LPT model, while $\chi^2_{\rm lin}$ is that for the linear theory, which doesn't take the BAO damping into account. In this computation, we haven't fitted any parameters, and the number of degrees of freedom is 19. $\chi^2_{\rm LPT} < \chi^2_{\rm lin}$ for all the models. This means that the models with the BAO damping match the observational results better.

No.	Ω_m	Ω_b	σ_8	n_s	b_0	α	$\chi^2_{\rm lin}$	$\chi^2_{\rm LPT}$	$\chi^2_{\rm simple}$
1	0.27	0.046	0.82	0.96	1.7	27.5	15.1	13.7	13.7
2	0.27	0.048	0.82	0.96	1.7	27.2	13.9	13.2	12.9
3	0.27	0.044	0.82	0.96	1.7	27.8	16.6	14.5	14.6
4	0.27	0.046	0.80	0.96	1.75	26.2	15.1	13.7	13.7
5	0.27	0.046	0.84	0.96	1.65	28.8	15.1	13.7	13.7
6	0.27	0.046	0.82	0.94	1.7	28.0	14.9	13.5	13.5
7	0.27	0.046	0.82	0.98	1.7	27.0	15.2	13.8	13.8
8	0.26	0.046	0.82	0.96	1.65	28.8	15.3	12.5	13.0
9	0.28	0.046	0.82	0.96	1.75	26.0	15.3	15.0	14.5

TABLE I. The results of the chi-square test for the BAO signature for various cosmological models. χ^2_{LPT} is based on the LPT power spectrum, while $\chi^2_{\rm lin}$ assumes the linear power spectrum. $\chi^2_{\rm simple}$ is the minimum chi-square value in fitting the model $B(k) = [1 - (d_* h^{-1}{\rm Mpc})^2 k^2] B_{\rm lin}(k)$.

§6. DAMPING OF THE BAO AS A PROBE OF THE GROWTH FACTOR

The damping of the BAO signature is closely related with the amplitude of the power spectrum, which is determined by $\sigma_8 D_1(z)$, while the BAO signature within the linear theory is determined by the density parameters $\Omega_m h^2$ and $\Omega_b h^2$. We discuss the feasibility of constraining $\sigma_8 D_1(z)$ by measuring the damping of the BAO in the power spectrum in quasi-nonlinear regime.

Figure 6 shows the 1σ error in measuring $\sigma_8 D_1(z = 0.9)$ as a function of $\bar{n}(b/2)^2$, where $\bar{n}$ is the mean number density of galaxies and b is the bias. This is evaluated by the Fisher matrix analysis assuming the the sample in the range of the redshift $0.5 < z < 1.3$ and the survey area ΔA. The thick (thin) solid curve assumes the sample with $\Delta A = 2000$ deg.^{2}($\Delta A = 4\pi$ radian). Here we adopted the fiducial target model is $\Omega_m = 0.28$ and $\sigma_8 = 0.82$, $\Omega_b = 0.046$, $h = 0.7$, and $n_s = 0.96$, which are the same as those adopted in figure 1. In this analysis the parameters other than $\sigma_8 D_1$ are fixed. Thus, the minimum attainable error of $\sigma_8 D_1(z = 0.9)$ of the WFMOS-like sample is 0.1 at the 1 sigma level, and smaller than 0.05 for the sample of $\Delta A = 4\pi$ steradian.

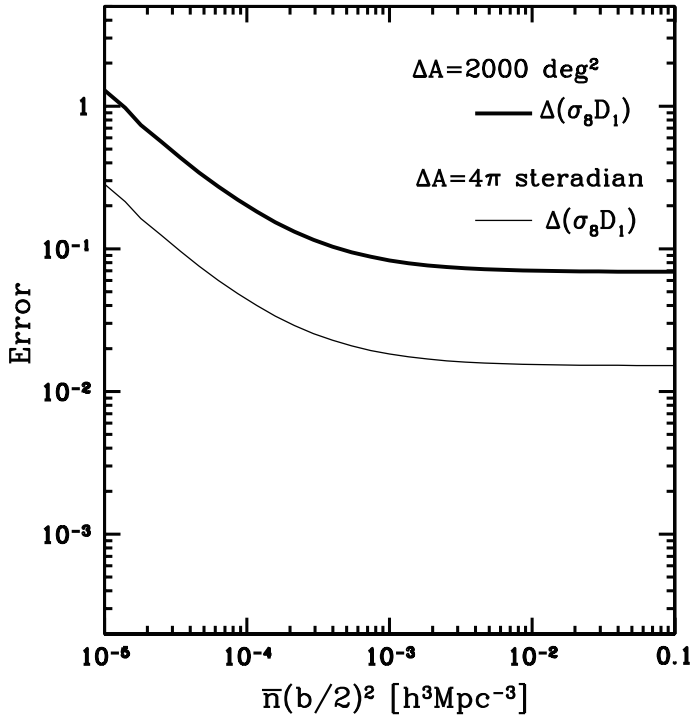

FIG. 6. The 1σ-level statistical errors of $\sigma_8 D_1(z=0.9)$ as a function of the number density $\bar{n}(b/2)^2$. The thick curves assume $\Delta A = 2000$ deg^2, and the thin curves assume $\Delta = 4\pi$ steradian.

§7. CONCLUSIONS

1. In the present work, we examined the effect of the nonlinear gravitational clustering on the BAO signature in the matter power spectrum. In particular, we focused on the damping of the BAO signature in the quasi-nonlinear regime. Our approach is based on the third order perturbation theory of the matter fluctuations, which enables us to investigate the damping in an analytic way. We found a simple analytic expression that describes the damping of the BAO signature, which clarifies what the important factor is for the damping. We showed that the leading correction for the damping is in proportion to the combination of $(\sigma_8 D_1(z))^2$.

2. We also discussed a possible extension of our formula to elaborate higher order nonlinear corrections using a technique of resumming infinite series of higher order perturbations on the basis of the Lagrangian perturbation theory developed by Matsubara [14], which incorporates the influence of the redshift-space distortions. This theoretical formula was compared with a result of N-body simulation, which showed the validity of the extended formula.

3. We confronted the theoretical BAO signature with the observed power spectrum of the SDSS LRG sample. The chi-squared test suggests that the observed power spectrum favours models with the BAO damping over the ones without the damping. Though the statistical significance is not high, the BAO damping has likely been detected in the SDSS LRG power spectrum. In our modelling we have not taken into account the effect of the clustering bias on the BAO damping. This should be considered more carefully in a future work.

4. A measurement of the damping of the BAO signature might be useful as a probe of the growth factor of the density fluctuations. As a first step to investigate such the possibility, we assessed the feasibility of constraining $\sigma_8 D_1(z)$ by measuring the damping of the BAO in the power spectrum. For a useful constraint, we need a very wide survey area of the sky.

[1] D. J. Eisenstein and W. Hu, Astrophys. J. **496** 605 (1998)
[2] A. Meiksin, M. White and J. A. Peacock, MNRAS **304** 851 (1999)
[3] D. J. Eisenstein et al., Astrophys. J. **633** 560 (2005)
[4] G. Hütsi, Astron. Astrophys. **449** 891 (2006)
[5] W. J. Percival et al., Astrophys. J. **657** 645 (2007)
[6] K. Yamamoto, Astrophs. J. **605** 620 (2004)
[7] http://www.sdss3.org/
[8] K. Glazebrook, et al.. arXiv:astro-ph/0701876
[9] B. . Bassett, R. C. Nichol & D. J. Eisenstein, arXiv:astro-ph/0510272
[10] L. Guzzo et al., Nature **451** 541 (2008)
[11] K. Yamamoto, T. Sato and G. Hütsi, Prog. Theor. Phys. **120** 609 (2008)
[12] H. Nomura, K. Yamamoto and T. Nishimichi, JCAP **0810** 031 (2008)
[13] H. Nomura, K. Yamamoto, G. Hutsi and T. Nishimichi, Phys. Rev. D **79** 063512 (2009)
[14] T. Matsubara, Phys. Rev. D **77** 063530 (2008)
[15] T. Nishimichi et al., Publ. Astron. Soc. Japan 61, pp.321-332 (2009)

APPENDIX LAGRANGIAN PERTURBATION THEORY

As a non-perturbative approach beyond the standard perturbation theory, Matsubara proposed a model of the quasi-nonlinear matter power spectrum using the technique of resuming infinite series of higher order perturbations on the basis of the Lagrangian perturbation theory (LPT) [14]. One of the advantages of using the LPT framework is the ability to calculate the quasi-nonlinear matter power spectrum in redshift-space, which can be obtained by

$$P^{(\mathrm{s})}_{\mathrm{LPT}}(k,\mu,z) = e^{-\alpha(\mu,z)D_1^2(z)g(k)}\Big[D_1^2(z)P^{(s)}_{\mathrm{lin}}(k,\mu,z) + D_1^4(z)P_2^{(s)}(k,\mu,z) + \alpha(\mu,z)D_1^4(z)g(k)P^{(s)}_{\mathrm{lin}}(k,\mu,z)\Big], \tag{14}$$

where

$$g(k) = \frac{k^2}{6\pi^2}\int_0^\infty dq P_{\mathrm{lin}}(q), \tag{15}$$

$$P^{(s)}_{\mathrm{lin}}(k,\mu,z) = \left(1+f\mu^2\right)^2 P_{\mathrm{lin}}(k), \tag{16}$$

$P_{\mathrm{lin}}(k)$ is the linear matter power spectrum at the present epoch, $f = d\ln D_1/d\ln a$, and $\alpha(\mu,z) = 1 + f(f+2)\mu^2$. $P_2^{(s)}(k)$ is expressed as

$$P_2^{(s)}(k,\mu,z) \;=\; P^{(\mathrm{s})}_{22}(k,\mu,z) + P^{(\mathrm{s})}_{13}(k,\mu,z), \tag{17}$$

where

$$P^{(\mathrm{s})}_{22}(k,\mu,z) = \sum_{n,m}\mu^{2n}f^m\frac{k^3}{4\pi^2}\int_0^\infty dr P_{\mathrm{lin}}(kr)\int_{-1}^1 dx P_{\mathrm{lin}}[k(1+r^2-2rx)^{1/2}]\frac{A_{nm}(r,x)}{(1+r^2-2rx)^2}, \tag{18}$$

$$P^{(\mathrm{s})}_{13}(k,\mu,z) = (1+f\mu^2)P_{\mathrm{lin}}(k)\sum_{n,m}\mu^{2n}f^m\frac{k^3}{4\pi^2}\int_0^\infty dr P_{\mathrm{lin}}(kr)B_{nm}(r), \tag{19}$$

and $A_{nm}(r,x)$ and $B_{nm}(r)$ are the function of r and x [14].